Materials and Design 30 (2009) 970–976

Contents lists available at ScienceDirect

Materials and Design

journal homepage: www.elsevier.com/locate/matdes

Investigation of the mechanical properties and microstructure of friction welded joints between AISI 4140 and AISI 1050 steels

Sare Celik *, Ismail Ersozlu

Department of Mechanical Engineering, Engineering and Architecture Faculty, Balikesir University, 10145 Balikesir, Turkey

ARTICLE INFO

Article history:
Received 18 April 2008
Accepted 30 June 2008
Available online 17 July 2008

Keywords:
C. Joining
D. Welding
F. Microstructure

ABSTRACT

Joining of dissimilar metals is one of the most essential needs of industries. Manufacturing with joint of alloy steel and normal carbon steel is used in production, because it decreases raw material cost. In this study, joining of AISI 4140 steel (medium carbon and low alloy steel) and AISI 1050 steel (medium carbon steel) was successfully achieved. Mechanical properties, macro and micro structural investigation of materials joined with this process were completed; joint strength was tested and optimum welding parameters were obtained. Moreover, temperature change of the weld zone was measured with an infrared temperature measurement device during welding; and the effects of the friction welding parameters on welding zone temperature were investigated. The highest tensile strength acquired in the welded specimens is 6% higher than parent AISI 1050 steel and the lowest tensile strength obtained was 1.9% lower than the parent AISI 1050 steel.

1. Introduction

Conventional fusion welding of many such dissimilar metal combinations is not feasible owing to the formation of brittle and low melting intermetallics due to metallurgical incompatibility, wide difference in melting point, thermal mismatch, etc. Solid-state welding processes that limit extent of intermixing are generally employed in such situations. Friction welding is one such solid-state welding process widely employed in such situations [1,2]. Main advantages of friction welding are high material saving, low production time and possibility of welding of dissimilar metals or alloys [3]. Nowadays; valves, bandix gears, axle shafts, gear-shaft components, turbocharged fan shafts, fork-shaft connections etc. in automotive industry are manufactured by the consolidation of alloy steel and normal carbon steel using friction welding process [4]. The most effective factors in the friction welding joining process are friction time t_f, friction pressure P_f, upset time t_u, upset pressure P_u, rotation amount n and the characteristic features of the welded material [5,6].

Sahin et al. [7] joined steel and copper using friction welding process in their studies. They determinated that maximum heat is away from the center, close to but not exactly at the surface during the welding process. Tjenberg [8] compared the calculated fatigue life with the tested life, for an embedded crack in the friction weld between two axially loaded rods. Lee et al. [9] explored the friction welding characteristics between TiAl and AISI 4140 steel in their studies. It was observed that martensite transformation occurred close to weld zone where volumetric growth had happened. Da Silva et al. [10] demonstrated that, besides friction welded titanium matrix composite (TMC) maximum tensile and yield strength provide good results even in high temperatures such as 200 and 375 °C, it also provides high strength-to-weight ratio. Arivazhagan et al. [11] have investigated the effects of welding parameters on the hot corrosion by joining AISI 4140 and AISI 304 steels through the friction welded method under molten salt of $Na_2SO_4 + V_2O_5$ (60%) environment at 500 and 550 °C under cyclic condition. Bayindir and Ates [6] developed a PIC controlled, laboratory sized friction welding machine in their studies. Joining of low carbon steel was accomplished with the designed device. In this study, joining of AISI 4140 steel (medium carbon and low alloy steel) and AISI 1050 steel (medium carbon steel) is successfully achieved. Accordingly, the objective of this study is to investigate the joint of AISI 4140 steel and AISI 1050 steel.

2. Experimental procedure

Controlled by the computer, constant driving friction welding machine (Fig. 1) with a maximum upset load capacity of 101,736 kN was used for implementing experimental study. A computer program was developed with Delphi 6 programming language for computer supervision and a control unit with a microcontroller (PIC16F84), which works on the data coming from the computer program, was designed and fabricated.

AISI 4140 and AISI 1050 steels, which are 10 mm in diameter and 80 mm in length, were used in the experimental studies. Tension test, hardness test (Table 1) and chemical analyses of the specimens (Table 2) were performed; and microstructures of parent metals

* Corresponding author. Tel.: +90 266 6121194; fax: +90 266 6121257.
E-mail address: scelik@balikersir.edu.tr (S. Celik).

0261-3069/$ - see front matter © 2008 Elsevier Ltd. All rights reserved.
doi:10.1016/j.matdes.2008.06.070

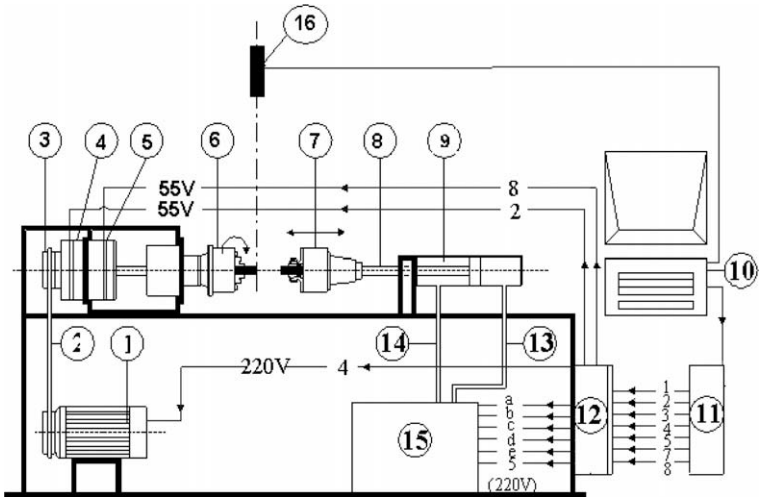

1. Main driving motor
2. "V" Belt
3. Pulley
4. Electromagnetic clutch
5. Electromagnetic brake
6. Chuck
7. Pliers
8. Piston arm
9. Dual affect hydraulic cylinder
10. Computer
11. Electronic control unit
12. Electric-control circuit
13. Pressure line
14. Return line
15. Hydraulic unit
16. Infra Red temperature measurement device

Fig. 1. Scheme of the continuous driving friction welding machine.

Table 1
Tensile strength and hardness of parent metals

Mechanical properties	AISI 4140	AISI 1050
Tensile Strength (MPa)	1059.7	1013.1
Hardness (Hv)	258	261

(Figs. 2 and 3) were researched before welding process. Pearlitic (P) and ferritic (F) structures are observed in AISI 1050 in Fig. 3.

Friction welding parameters of the AISI 4140 and AISI 1050 steels were obtained from the literature [9] and the preliminary work. In this study, upset time (t_u), upset pressure (P_u) and rotational speed were fixed at 14 s, 162 MPa and 3000 rev/min, respectively, while

Table 2
Chemical composition of parent metals (wt%)

Element (wt%)	Fe	C	Mn	Si	P	S	Cr	Mo	Co	Nb<	Ni	Ti	Al	Cu	V	W<	Pb>
AISI 4140	97.318	0.417	0.772	0.260	0.008	0.005	0.923	0.157	0.006	0.002	0.051	0.002	0.029	0.050	0.003	0.002	
AISI 1050	97.839	0.481	0.675	0.221	0.008	0.037	0.220	0.015	0.004	0.004	0.042	0.001	0.018	0.090	0.004	0.004	0.030

Fig. 2. Optic microstructure of AISI 4140 steel.

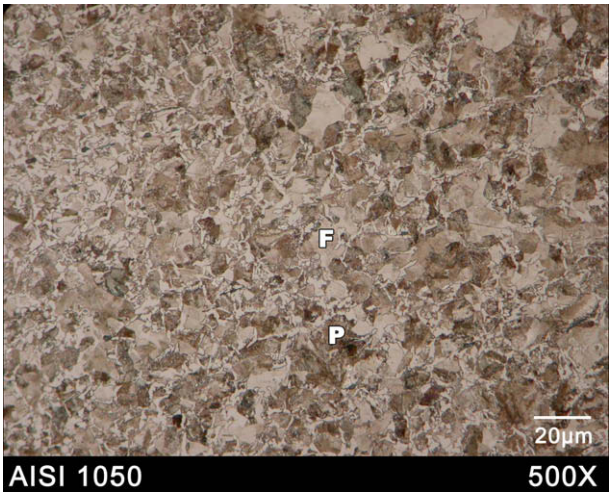

Fig. 3. Optic microstructure of AISI 1050 steel.

Table 3
The process parameters used in the friction welding experiments

Specimen no.	Friction time (s)	Friction pressure (MPa)	Flash width 4140 (mm)	Flash diameter 4140 (mm)	Flash width 1050 (mm)	Flash diameter 1050 (mm)
Specimen 1	6	81.00	2.60	14.50	3.20	15.60
Specimen 2	6	121.5	4.70	16.40	5.90	17.30
Specimen 3	6	162.00				
Specimen 4	4	121.50	3.70	15.00	5.00	16.00
Specimen 5	4	162.00	4.40	15.80	5.80	16.40
Specimen 6	4	202.50				
Specimen 7	8	81.00	3.85	15.80	4.40	17.20
Specimen 8	8	121.50	5.70	17.20	6.80	18.30

friction time (t_s) and friction pressure (P_s) values were altered as given in Table 3. Five experimental applications were carried out for each set of welding parameters. The diameters and widths of the flashes were also measured and are presented in the same table.

Tensile properties and hardness values of the welded specimens were measured. Microstructures and chemical structures of the welded specimens were examined, by using optic and scan electron microscope (SEM) and energy dispersive spectroscopy (EDS) analyzer, respectively. Temperature of the welded zone was measured and optimum welding parameters were obtained.

3. Results and discussion

3.1. Tensile properties

Friction welding experiments were accomplished successfully using determined welding parameters. During tensile tests, brittle break off occurred at AISI 1050 steel in specimens 2–8 (Fig. 4); ductile break off occurred at AISI 4140 steel in specimen 1 (Fig. 5). Tensile strength of the welded specimens was very close to that of the parent material, AISI 1050 steel (Fig. 6). Tensile tests applied on welded specimens revealed that friction time and friction pressure, which are friction welding parameters were effective on joint strength. The highest tensile strength was acquired as 1073.9 MPa in welded specimen 1 and the lowest tensile strength was obtained as 993.9 MPa in specimen 6.

When friction pressure is superfluous in specimen 6, volume of viscous material transferred at the weld interface decreases as a re-

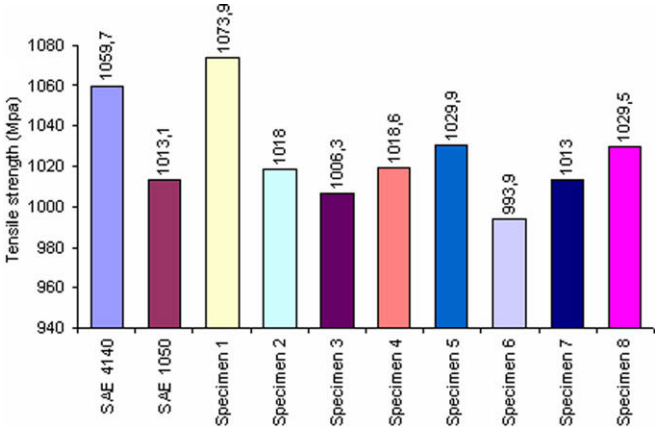

Fig. 6. Tensile strength of welded specimens.

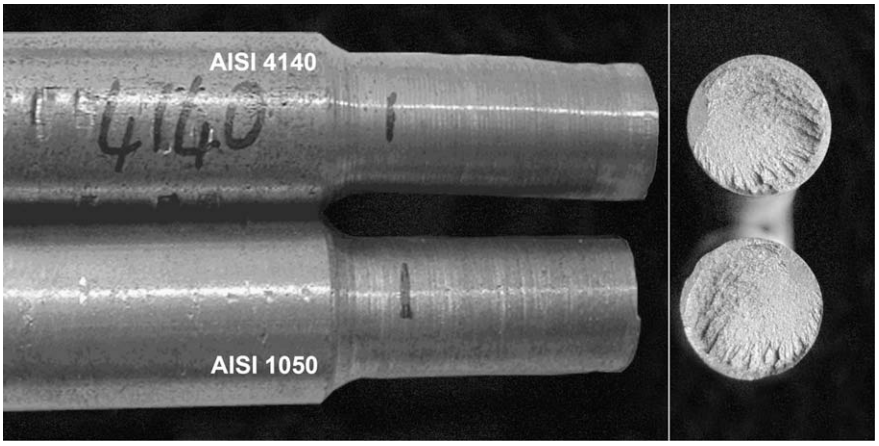

Fig. 4. The macro photographs of the tensile tested and the brittle fracture surface of tensile tested specimen.

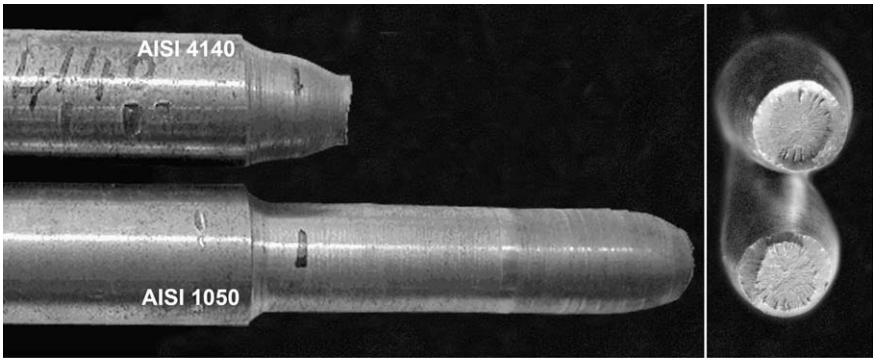

Fig. 5. The macro photographs of the tensile tested and the ductile fracture surface of tensile tested specimen.

sult of more mass discarded from the welding interface, which resulted in lower tensile strength. In specimen 1, optimisation of friction pressure and friction time increased the volume of viscous material transferred at the weld interface, which resulted in higher tensile strength.

The highest tensile strength acquired in the welded specimens was 6% higher than parent AISI 1050 steel whose tensile strength was 1013.1 MPa and the lowest tensile strength obtained was 1.9% lower than parent AISI 1050 steel.

3.2. Hardness test results

Hardness tests of the welded specimens were implemented on horizontal direction in Vickers scale (Fig. 7). Hardness value obtained in the weld zone was much higher than the hardness of the parent materials. The reason for this increase in hardness at the weld zone was the creation of carbide by the alloy elements of chrome and molybdenum [12] and grain size reduction of the particle structure (Fig. 8) during the consolidation of alloy steel and normal carbon steel under the circumstances of high temperature and high pressure.

Transformed material varied according to welding parameters in the welding zone. Transformed material resulted in the increase of C diffusion and Cr transfer. This fact led to a martenzitic structure in these zones and an increase in hardness value. The situation described here brought about the fact that maximum hardness occured on AISI 4140 side of the weld for sepcimens 1, 7 and 8.

While moving from the weld zone to the base material through the HAZ, hardness value varies according to welding parameters. In AISI 1050 steel, the hardness value obtained at 1mm from the weld zone is slightly lower than that of the base material. The reason for this difference was the decrease of Cr and Mn ratio, which is seen in EDS analysis. In AISI 4140 alloy steel, the hardness value obtained at the heat affected zone was registered higher than that of the base material. The reason for this difference was the increase of Cr ratio and martenzitic structure, which is seen in EDS analysis and Fig. 8c.

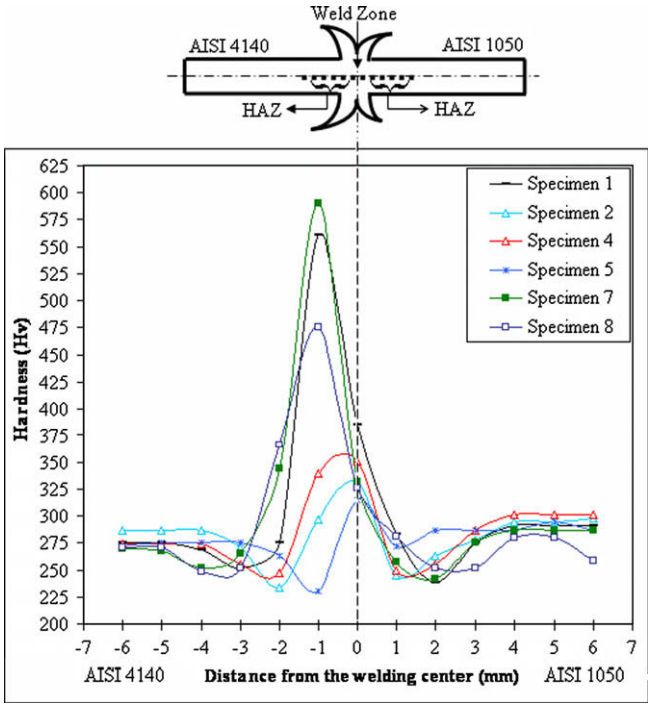

Fig. 7. Hardness variations on horizontal distance.

3.3. Macro and microstructure

The macrostructures of the weld zone and the heat affected zone are shown in both Figs. 9 and 10. Depending on the angular velocity, in the weld zone, temperature at the centre is minimum, while the temperature at the circumference is maximum. It was observed that structural change takes place in relation to this temperature change [7].

In the case of dissimilar materials joints by friction welding, the formation of the flash depends on the mechanical properties of two parent materials [9]. It was observed that the flashes were formed around the weld interface on sides of both AISI 4140 and AISI 1050 steels (Fig. 11). The amount of flash increased with increasing t_s, P_s and P_u. The average flash diameter formed in AISI 1050 steel was measured to be 6.46% more than that of AISI 4140 steel and the average width of flashes formed in AISI 1050 steel was measured to be 24.84% more than that of AISI 4140 steel (Table 3).

In the optical microscope observation of all welded specimens, due to the effect of pressure and heat, grain size reduction has been observed at the HAZ's of both base materials (Fig. 8).

Microstructure inspection of the weld zone (Fig. 12), heat affected zone of AISI 4140 steel (Fig. 13) and AISI 1050 steel (Fig. 14) were made via SEM. It is observed during SEM inspection that there are no cracks or blank spaces and the transition of materials between AISI 4140 steel and AISI 1050 steel in the weld zone (Fig. 12). During the friction welding process, the temperature near the weld interface would reach between A_3 temperature and the melting point of AISI 4140 steel. Therefore, the microstructure of AISI 4140 steel was transformed to the austenite. The austenite microstructure was changed to the other phases due to the diffusion of carbon to the grain boundary and rapid cooling rate [13]. When exposed to cooling from elevated temperatures, the AISI 4140 steel experienced a martensite transformation near the weld interface of AISI 4140 steel (Fig. 13) [9,13]. Pearlitic structure was observed (Fig. 14) at the heat affected zone of AISI 1050 steel [14].

3.4. EDS analysis

EDS analyses were performed at five points, which are given at Fig. 15, on welded specimens and results of the chemical analyses are given in Table 4. During welding, transition of materials at the weld zone occurred due to temperature and pressure. Mn ratio increased too much at (a), (b), (c) and (d) points but at (e) point it did not increase that much. Cr ratio decreased on AISI 1050 steel side and increased at the weld zone and AISI 4140 steel side (Tables 2 and 4). From these tables it is observed that chromium diffuses towards low alloy steel from the medium carbon steel side This situation stands parallel to the hardness distribution of the welded specimens (Fig. 7).

3.5. Temperature analysis

The temperature of the weld zone was measured using infrared temperature measurement device during welding process. Temperature–time graph regarding welded specimens are given in Fig. 16. It is seen that heat increases rapidly within the first 2 s when the graph is examined (800–900 °C). From that point forward, even though the rotation and friction pressure resumes, the temperature rising speed slows down. The reason for this situation is the decrease of the friction coefficient caused by the warming up of the specimens [15] and the existence of the plastic deformation. Applying different friction pressures affected the reaching time of different welding temperature levels, which is proportional to the increase of pressure. It is ob-

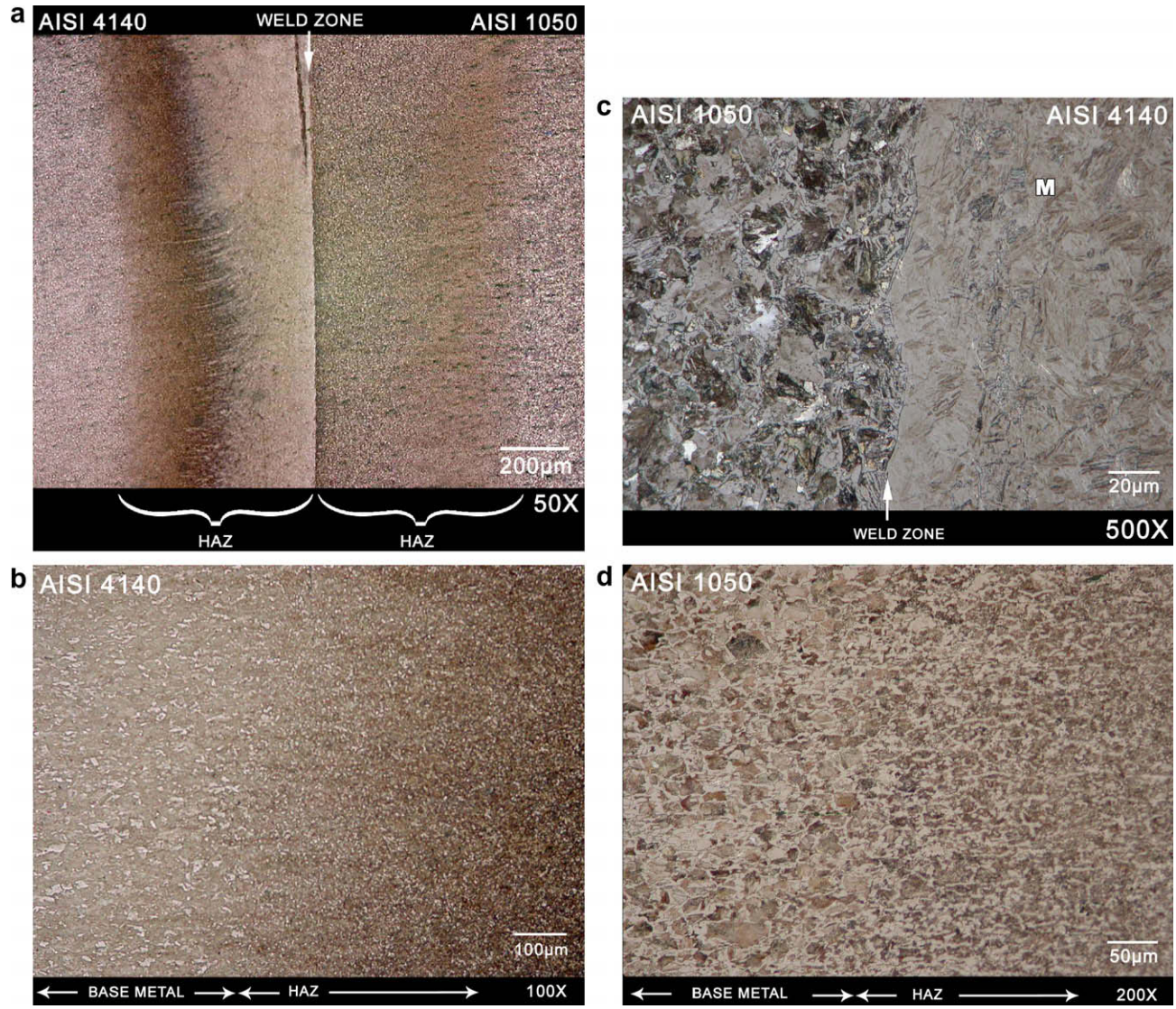

Fig. 8. (a) Optic microstructure of welded specimen, (b) optic microstructure of HAZ on AISI 4140 steel, as welded, (c) optic microstructure of weld zone and (d) optic microstructure of HAZ on AISI 1050 steel, as welded (Specimen 1, P_s = 81 MPa, t_s = 6 s, P_u = 162 MPa and t_u = 14 s).

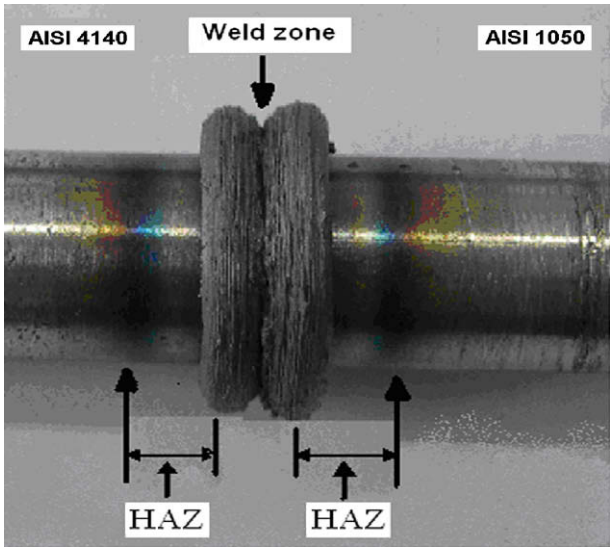

Fig. 9. Photo of welded specimens.

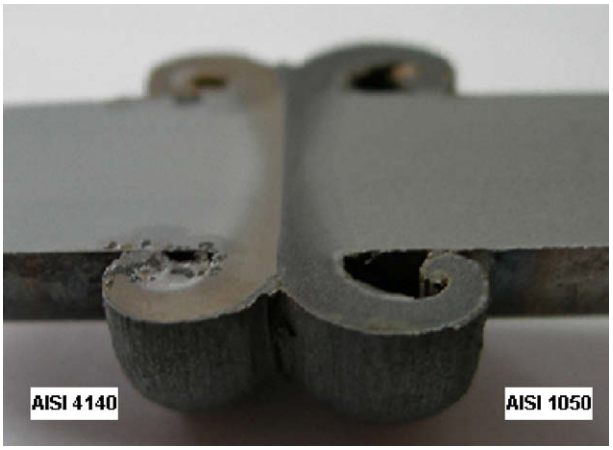

Fig. 10. Macro-photograph of joint, as welded.

served that the maximum weld temperature did not exceed the hot deformation temperature (1100 °C for AISI 1050 steel). But after reaching the maximum weld temperature, continuous friction pres-

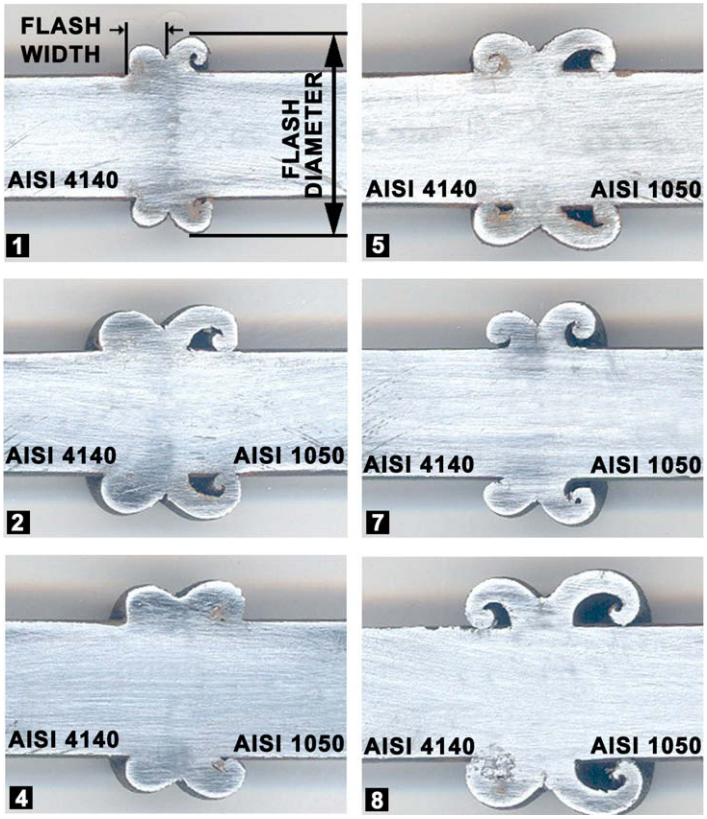

Fig. 11. Macro photographs of flashes formed in welded specimens.

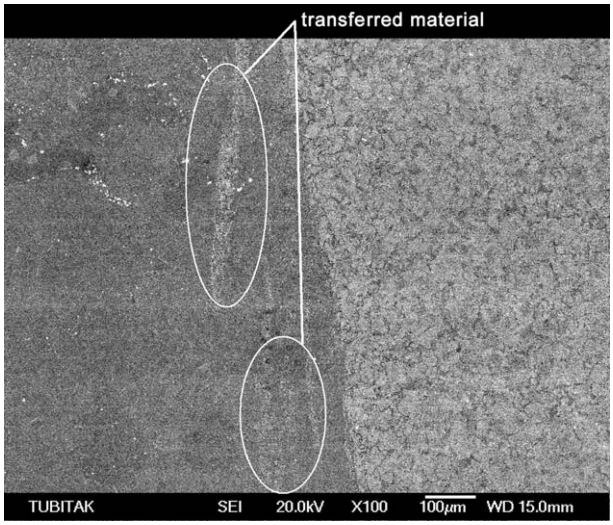

Fig. 12. SEM microstructure of the weld zone (Specimen 1).

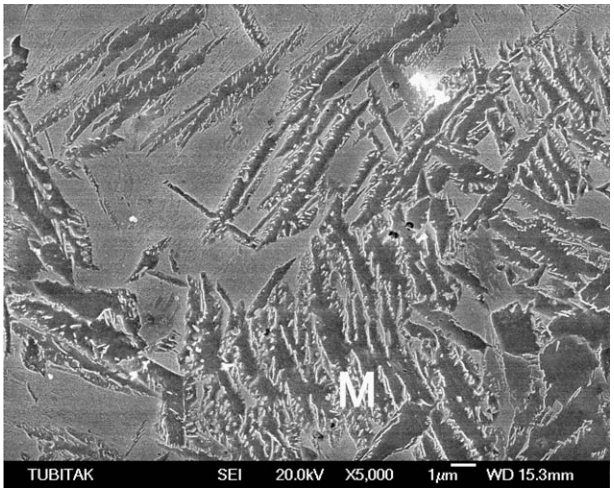

Fig. 13. Microstructure of HAZ on AISI 4140 steel, as welded (Specimen 1).

sure and rotational process increase the deformation of the specimens. It is examined that two friction welding parameters, which are friction pressure and friction time, affected the heat of the weld zone significantly.

4. Conclusions

The following are the important results in this work:

(i) Joint of the AISI 4140 steel (medium carbon and low alloy steel) and AISI 1050 steel (medium carbon steel) was achieved successfully using friction welding method. The tensile strength of the welded specimens was detected very close to that of parent materials. Hardness of the weld zone was obtained higher than the hardness of that of parent materials. Hardness value of the HAZ varied according to the welding parameters.

(ii) There were no cracks or blank spaces in optical and SEM observations. Grain size reduction occurred at the HAZ's of both base materials. It was observed that transition of materials at the weld zone occurred in SEM inspection and EDS analyses.

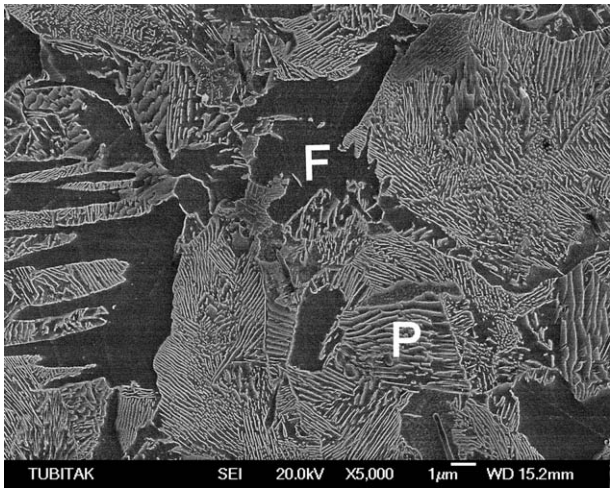

Fig. 14. Microstructure of HAZ on AISI 1050 steel, as welded (Specimen 1).

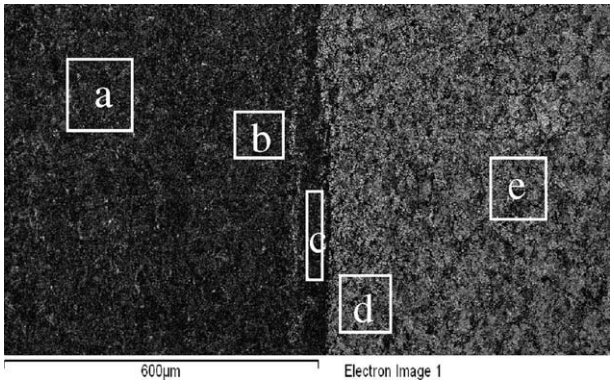

Fig. 15. EDS analysis of the five points: (a) and (b) HAZ of AISI 4140; (c) weld zone; (d) and (e) HAZ of AISI 1050.

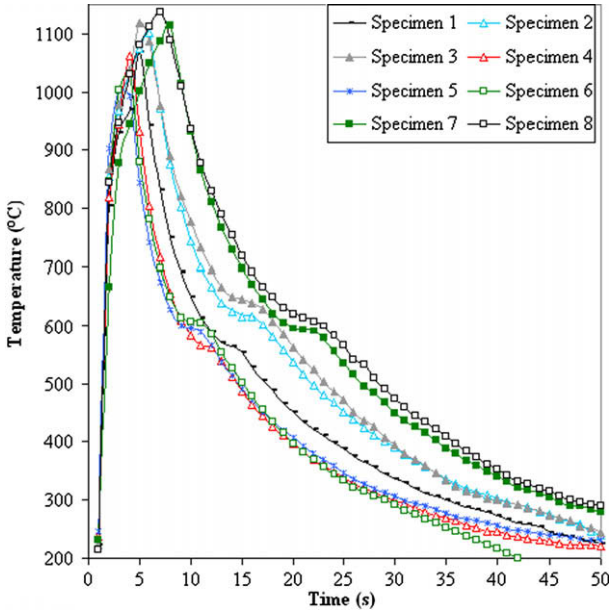

Fig. 16. Temperature graph of the weld zone.

Table 4
EDS data of the five points, as welded

Element	(a) AISI 4140 (wt%)	(b) AISI 4140 (wt%)	(c) Welding zone (wt%)	(d) AISI 1050 (wt%)	(e) AISI 1050 (wt%)
Cr K	1.13	1.28	1.16	0.03	0.10
Mn K	1.07	1.06	1.43	1.17	0.87
Fe K	97.52	97.39	97.19	98.54	98.88
Ni K	0.27	0.26	0.22	0.26	0.15

(iii) Temperature increase within the first 2 s takes place rapidly at the weld zone. From that point forward, even though the rotation and friction pressure resumes, the temperature rise slows down.

(iv) Optimum welding parameters determined in the experimental studies conducted, namely rotation speed, friction pressure, friction time, upset pressure and upset time were obtained as 3000 rev/min, 81 MPa, 6 s, 162 MPa and 14 s, respectively, in the joining process of AISI 4140 steel and AISI 1050 steel using friction welding process.

Acknowledgements

University of Balikesir, Institute of Science, Department of Mechanical Engineering, Land Forces N.C.O Vocational High School Department of Technical Science and 1012 Main Repair Factory contributed to this study. Authors render thanks to all of these institutions.

References

[1] Meshram SD, Mohandas T, Madhusudhan Reddy G. Friction welding of dissimilar pure metals. J Mater Process Technol 2008;184:330–7.
[2] Sathiya P, Aravindan S, Noorul Haq A. Some experimental investigations on friction welded stainless steel joints. Mater Des 2007;29:1099–109.
[3] Sahin M. Simulation of friction welding using a developed computer program. J Mater Process Technol 2004;153(4):1011–8.
[4] Chalmers RE. The friction welding advantage. Manuf Eng 2001;126:64–5.
[5] Alvise LD, Masoni E, Wallve SJ. Finite element modelling of the inertia friction welding process between dissimilar materials. J Mater Process Technol 2002;125(6):387–91.
[6] Bayindir R, Ates H. Low-cost and high sensitively microcontroller based control unit for a friction welding machine. J Mater Process Technol 2007;189:126–31.
[7] Sahin AZ, Yibas BS, Ahmed M, Nickel J. Analysis of the friction welding process in relation to the welding of copper and steel bars. J Mater Process Technol 1998;82:127–36.
[8] Tjernberg A. Fatigue life of a friction welded joint with a circular crack in the center. Eng Failure Anal 2000;7:221–7.
[9] Lee WB, Kim YJ, Jung SB. Effects of copper insert layer on the properties of friction welded joints between TiAl and AISI 4140 structural steel. Intermetallics 2004;12:671–8.
[10] Da Silva AAM, Meyer A, Dos Santos JF, Kwietniewski CEF, Strohaecker TR. Mechanical and metallurgical properties of friction-welded TiC particulate reinforced Ti–Al–4V. Compos Sci Technol 2004;64:1495–501.
[11] Arivazhagan N, Singh S, Prakash S, Reddy GM. High temperature corrosion studies on friction-welded dissimilar metals. Mater Sci Eng B 2006;132:222–7.
[12] Chenje TW, Simbi DJ, Navara E. Relationship between microstructure, hardness, impact toughness and wear performance of selected grinding media forb mineral ore milling operations. Mater Des 2004;25:11–8.
[13] Lakhkar Ritesh S, Shin Yung C, Krane Matthew John M. Predictive modeling of multi-track laser hardening of AISI 4140 steel. Mater Sci Eng A 2008;480:209–17.
[14] Lyman T. Atlas of microstructures of industrial alloys. Metals handbook, vol. 7. ASM; 1972. p. 39.
[15] Labthink Instruments Co. Material friction coefficient and temperature <http://www.labthink.cn/service/show558.html>; 2006.